Coherent Marine Radar Measurements of Ocean Surface Currents and Directional Wave Spectra

Dennis B Trizna
Imaging Science Research, Inc.
6103B Virgo Court
Burke, VA 22015 USA

***Abstract*- A coherent marine radar with 3-m resolution has been developed that measures the radial component of the orbital wave velocity of ocean waves, as well as the mean radial ocean surface velocity. This radar allows direct measurement of the ocean wave spectrum by means of 3D-FFT processing of a sequence of coherent radar images of orbital wave patterns. Currently, with a 2.5-s rotation rate, 256 images cover a period of the order of ten minutes, with frequency alias at 0.2 Hz, with upgrade to 0.4 Hz planned with later units. Radial current maps are obtained by a superposition of all radial velocity images collected. This summing forces orbital wave patterns to blend to the mean, resulting in the map of mean radial current. A pair of such radars operated at a coastal site, separated by a few hundred meters along the coastline, may allow the combination of 2-site radial components to be combined into a mean current vector field. Results of first tests of the first prototype radar measurement of radial current and RMS wavehieght are presented for a field site at the U.S. Army Corps of Engineers Field Research Facility, Duck, N.C.**

I. OMEGA-K SPECTRA

Marine radar offers a snapshot sequence every 1.25 to 2.5 s of the coastal wave field that can be used for the application of a number of image processing algorithms. A number of researchers have established the utility of using both radar and optical video image sequences to derive useful coastal ocean properties from such data [1-6]. We fave recently developed an integrated radar and data acqusition package to make such measurements synoptically and unattended. The prototype system has been set up at the U.S. Army Corps of Engineers Field Research Facility (FRF), Duck, NC for extensive testing and ground truth comparison. Real time results can be viewed at the FRF website (frf.usac.army.mil/radar). The coherent marine radar processing is very similar to that of the non-coherent version, as maps of ocean waves are also created. However, in the case of the standard marine radar, the image is one of backscatter intensity. For the coherent marine radar, the image will be the radial component of orbital wave velocity, that will represent traveling ocean wave orbital wave velocity maps. As the processing is similar for both cases, we first present the general approach used for the standard marine radar.

II. COHERENT RADAR DESCRIPTION

Use of non-coherent marine radar for ocean wave spectra measurement is feasible by making use of multiple-rotation images, and 3-D FFT image processing to derive Ω-K ocean wave spectra [1-7]. We have developed a similar capability, based on the Sitex family of marine radars. The coherent radar has a similar look to standard marine radars, as seen below, for such a system currently operating at the USACE Field Research Facility, at Duck NC shown in Fig. 1 below.

Figure. 1. ISR coherent marine radar used for wave sensing.

The radars used for the results presented here are two . The first is our coherent-on-receive ISR CORrad Digital Imaging Radar Model 25.9, based on a modified Koden 25-kWatt 9' antenna system, with our digital acquisition system and signal processing systems, Radar Image Processing Suite (RIPS). A fully coherent prototype radar (COHrad) was developed in house, and a new solid state transceiver just delivered for our commercial version. With suitable processing, the COR IF signal can be used to retrieve coherent estimates of radial velocity similar to CORrad, as will be demontrated later. A photo of the solid state module, including 5-watt power amplifier, is shown in Fig. 2.

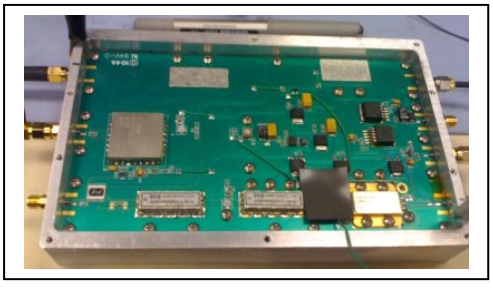

Figure 2. Solid state transceiver module.

The radar makes use of pulse compression to achieve improved gain over the standard marine radar, allowing it to operate with just 5-watts of peak power. A 1-µs pulse that is transmitted is shown in Fig. 3a below, chirped over 30 MHz in this case, and mixed up to X-band for transmission. Echoes have a similar shape and pulse compression correlation creates in-phase (I) and quadrature (Q) samples that are used for velocity measures. These are shown in Fig. 3b and 3c below.

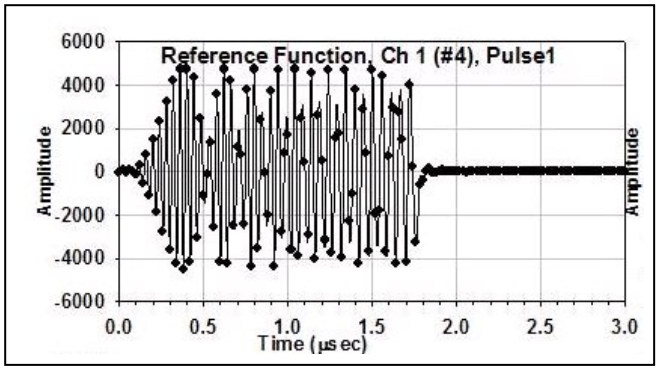

Figure 3a. Chirped pulse transmitted, after mixing to X-band.

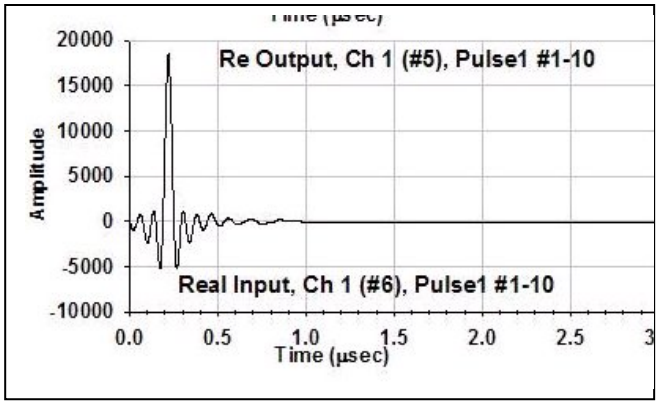

Figure 3b. In-phase pulse compressed echo using 3a.

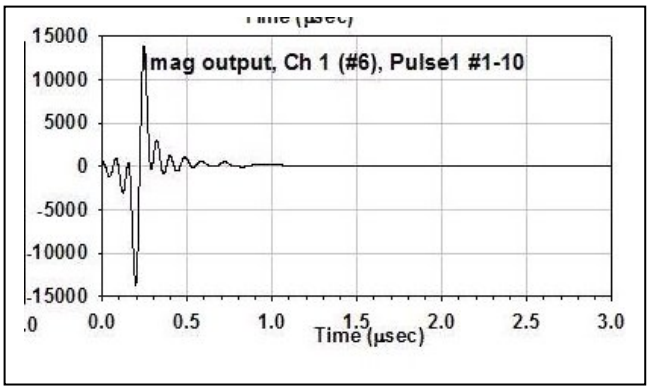

Figure 3c. Quadrature signal (90 deg out of phase with I).

The phase at each time sample is determined from the equation ATAN(I/Q), and a phase difference, dϕ, from two consecutive pulses is calculated for each range sample. This is proportional to the radial velocity using the Doppler equation, $v = d\phi / (\lambda/2)$. The range-azimuth matrix of radial velocities are then transformed into Cartesian co-ordinates for each rotation of the radar. The radar video echo intensity signal, $S(R.\phi)$, can be formed at each pixel for comparison using $S(R.\phi) = (I^2+Q^2)^{1/2}$. A map of images of intensity and radial velocity is shown below in Fig. 4a and 4b.

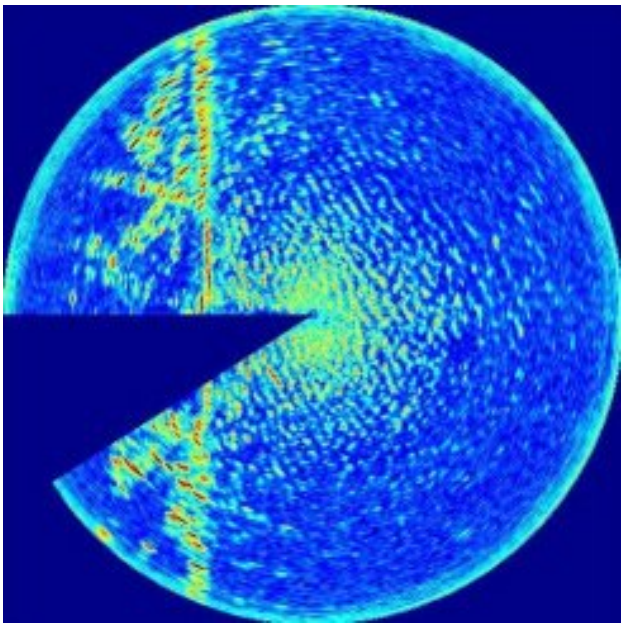

Figure 4a. Radar echo intensity image.

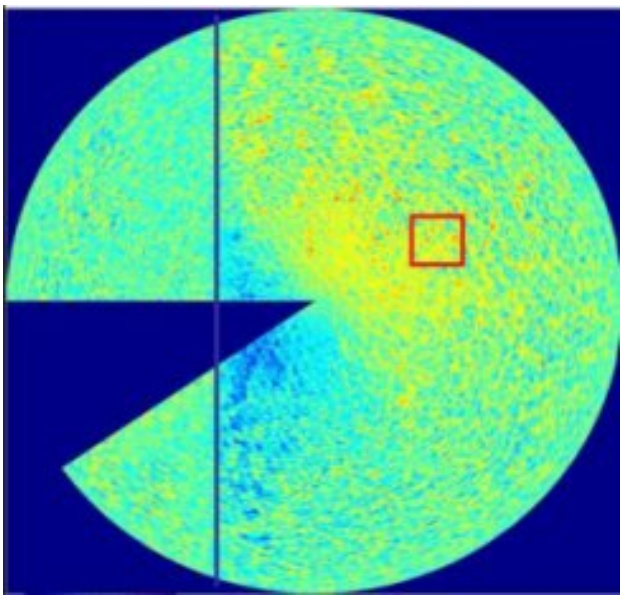

Figure 4b. Radial velocity image.

The radial velocity map appears to show usable information at ranges where the intensity signal is weak, but stil provides quality I/Q values to allow phases to be determined. There is an offset due to current here that will be discussed later. The red box represents a user-selectable set of pixels that can be chosen for successive rotations to

be used as input to a 3D-FFT analysis that is used to determined values of spectral samples of waveheight-squared/Hz. This window can be moved about the radar coverage scene to study wave dissipation, for example, or wave refraction spectra in unusual bathymetry environments. One must correct for the radar aspect relative to the primary wave direction, as the radar radial component will vary like cosine of the difference of wave travel vs radar illumination.

III. OMEGA-K SPECTRA

Fig. 5 represents a subset of frequency spectra from a set of 32 that are available when using 64 rotations of 64x64 pixels, then averaging over 8 of such sets covering a 10-min period. The yellow circle seen represents the shallow water dispersion rule for the depth chosen, 10 m, while the red circle represents deep water.

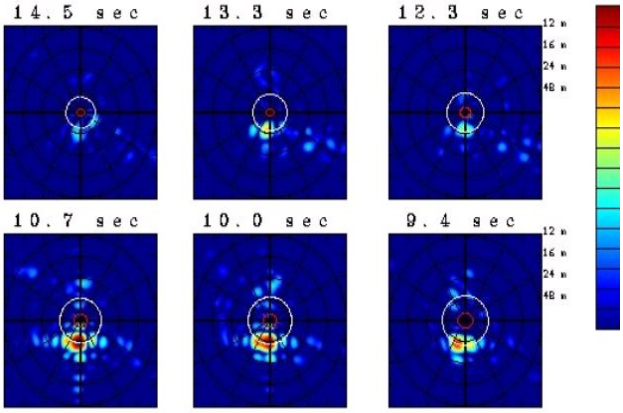

Figure. 5. K_x-K_y Spectra at each of a series of wave frequencies from the Ω-K spectral analysis.

The spectral peaks clearly lie on the shallow water dispersion circle chosen, and each image can be filtered using a band between 80% and 120% of this radius, to account for tidal changes in depth. All energy in this band will represent samples of wave height squared per unit Hz, (0.4Hz/64 in this case). This is obtained by relating the radial velocity from the radar measure to the spectral waveheight component using the time derivative of the equation defining the x-position of a patch of water on a wave surface :

$$X(t) = (H/2)\cos(\Omega t) \qquad (1)$$

In the case of processing the intensity image of a standard marine radar, similar image intensity spectra result, but each radar frequency component must be scaled to some surface truth representation of the weave frequency spectrum using an emprical constant, a spectral Modulation Transfer Function. This has shown to be in error when environental conditions change (wind direction relative to wave direction, for example), and if the radar modulator ages with time and exhibits chaning output power. The coherent radar approach requires no such scaling, and is independent of such environmental factors. A patent based on this approach has been applice for by ISR and is pending, and an international provisional patent has also been filed.

IV. FREQUENCY SPECTRA AND H_m0

If one sums the spectral energy in the band about the shallow water dispersion relation for each of 32 windows, one derives an omni-directional freqeuency spectrum. A comparison of that derived from coherent radar data over 10 minutes, and the pressure array sensor at the FRF for two overlapping periods of 3-hr each is shown in Fig. 6 below.

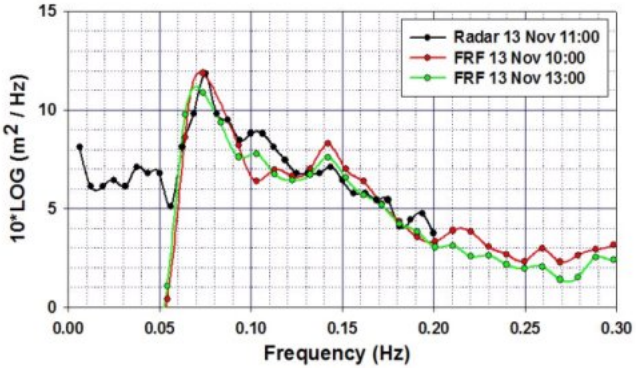

Figure 6. Frequency spectra from COHrad and FTF pressure array.

If one sums the energy from each spectral peak in the frequency spectrum above, one forms H_m0, a RMS waveheight estimate. During November of 2009, Hurricane Ida passed offshore of the FRF site and waves of 4-m were observed. Below are plotted the time series of H_m0 from the radar vs that from the FRF pressure sensor array.

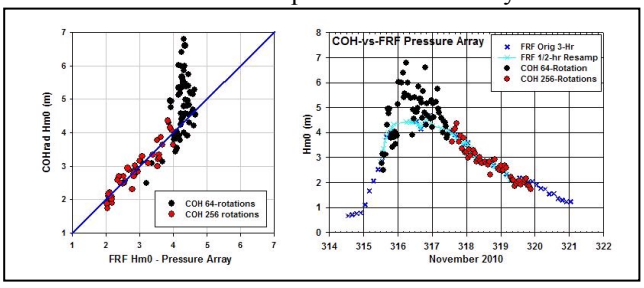

Figure 7. Hm0 time series from radar vs FRF pressure array compared.

The black circles represent very short times of collections, just 64 rotations covering ~2.5 minutes, enought for a single 3D-FFT analysis. As the winds subsided but the waves still being high, the collections were increased to 256 rotations, represented by the red circles. The agreement is quite good for these conditions and illumination into waves offshore of the pier end. It suggests that at least ten minutes of radar

data are required for a suitably stable Hm0 retrieval.

The CORrad was run simultaneously from the same location a frew meters away and processing that data in a similar fashion produced results for Hm0 as well. These are shown in Fig. 8 below.

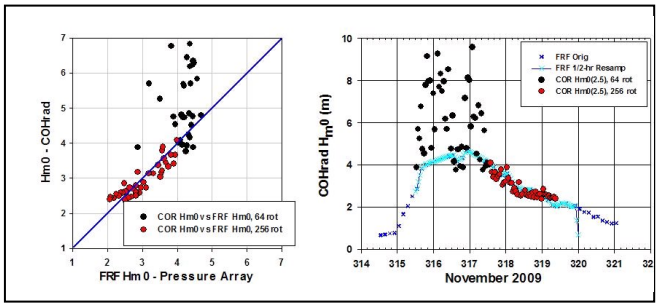

Figure 8. CORrad Hm0 vs FRF pressure array results

The results from the CORrad system are quite similar to those of the COHrad for the same period, and the need for more than 64 rotations of data are apparent here as well.

A third radar was operated at a different time in 2010, from a location on shore instead of the end of the pier. This is a scenario that is more likely for most potential applications. This was data from a CORrad as well, running over 512 rotations at twice the rotation rate of the COHrad, so covering the same 10-min or so time period. The height of the antenna was lower than that at the end of the pier, atop a 32' telescoping tower on ~3-m mean height behind the dune at the FRF site. They were collected at relatively short range, 384 m offshore, as onley 512 range samples were collected, and compared with FRF data from ~800 m offshore.

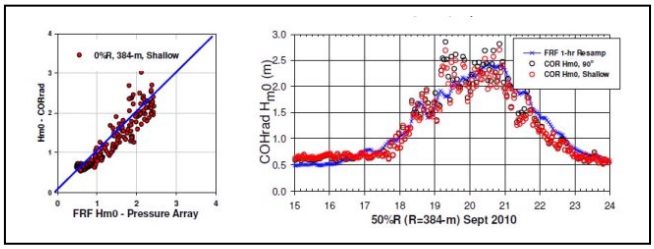

Figure 9. CORrad data from a shore site.

In this case, the results show the effect of the depth change with tidal cycle for the higher eave conditions, which was not accounted for. Nonetheless, the comparison is quite good for this shore side location.

V. RADIAL SURFACE CURRENTS

As discussed earlier, if one takes the mean of the sum of all radial velocity images, in the absence of severe shadowing of the wave troughs by wave crests for steep wave conditins and modest to high waves, one can derive radial surface currents from either type of radar discussed here. Fig. 10 below shows an example of 256 rotations summed for both radial velocity and magnitude images for the COHrad system during the Nov 2009 storm.

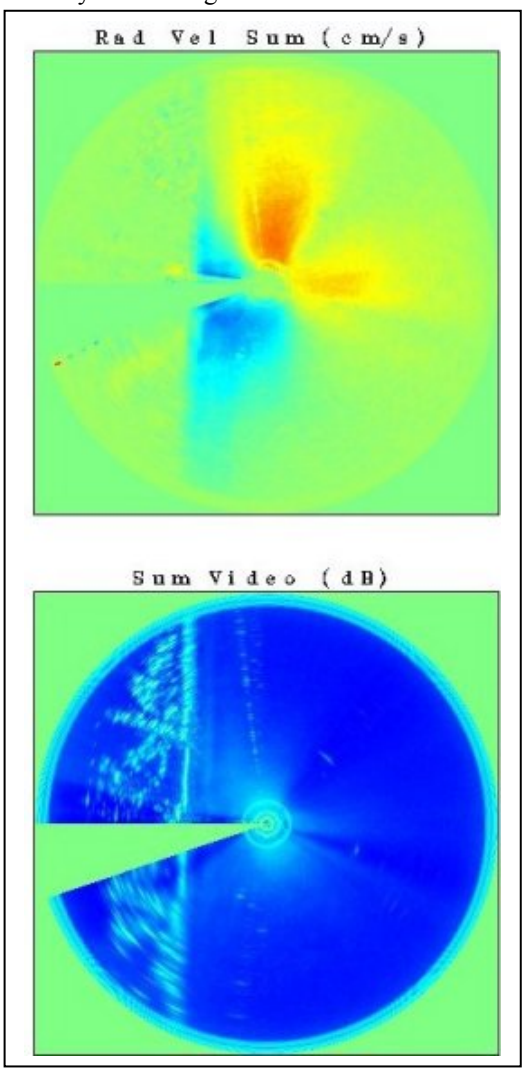

Figure 10. Summed radial velocity (top) and intenssity (bottom). The gap in the upper right quadrant of the redial velocity image is due to shadowing of the radar beam.

The maximum range extent in this case is about 700 m for the 1.5 km radar coverage (the pier is 600 m offshore). The drop off in radial velocity is thought to be due to the onset of shadowing, but has not been investigated thuroughly. Recent tests using a 19-m radar height was able to image currents out to 3-km range, so radial current measure is dependent on antenna height.

As the radar was turned during the experiment, it was difficult to make comparisons directly over surface truth currents from bottom mounted acoustic sensors that gave

vector values. Instead, we calculated currents over a range-azimuth ring, summing between 250-250 meters range extent, then over 10 adjacent azimuthal bearings of the 595 that were avialable. The maximum value in azimuth was determined to be a measure of maximum mean current. The acoustic Doppler vector currents were used to get a magnitude time history as well and these were compared. Because the maximum radar current magnitude was not necessarily at the same range-azimuth as the 5-m acoustic sensor, nor at the same depth, the comparisons should be taken with a grain of salt. The results of such a comparison is shown in Fig. 11.

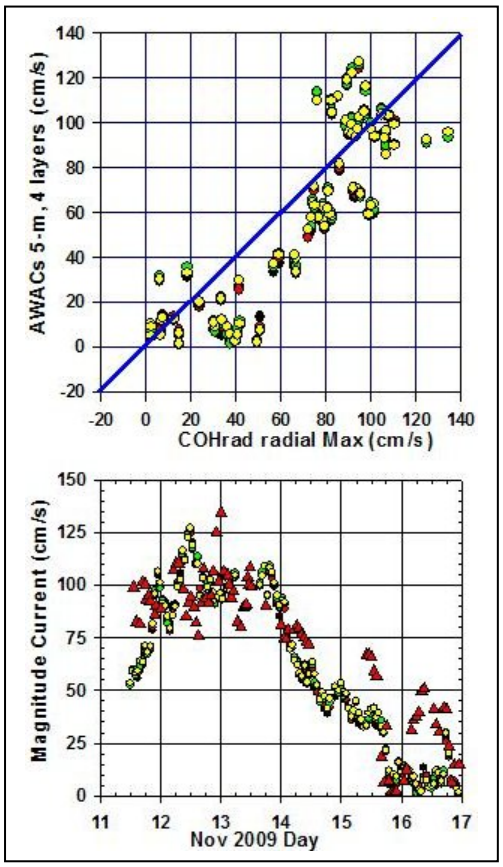

Figure 11. Time series of COHrad current magnitude (red triangles) and 3 acoustic depths near the surface, with scatter diagram comparison.

VIII. SUMMARY

We have demonstrated the use of a newly designed coherent marine radar to measure directional wave spectra and surface radial currents. Data were compared with surface truth instrumentation from the USACE Field Research Facility, both pressure array sensor data for wave height, and AWAC acoustic sensors for currents. Data from a coherent-on-receive radar that was run simultaneousl from the end of the pier at the FRF and compared favorably as well. For this location, currents along shore can be measured reasonably accurately for the modest radar height of roughly 11 m, as the radar is looking along the crests and troughs and does not suffer shadowing, even for modest to low radar height for this geometry. Looking offshore, the troughs would be shadowed by the crests for very steep waves, and the orbital wave velocity would not present a zero mean to the radar look. We found this to be the case for a shore based radar on another occasion, where the currents were in error due to crest orbital wave influences. For this case, the wave height analysis was still quite respectable. On more recent observations at other sites with radar heights ranging from 19 m to 26 m, no shadowing was encountered and long range currents could be measured accurately.

A pair of radars discussed here, placed of the order of 300 to 1,000 m apart, should be able to provide a vector map of surface currents at 3-m resolution. Such a method should be useful for detection of rip currents and riverene flow, in addition to currents in harbors for ship traffic application.

ACKNOLEDGEMENTS

We wish to acknowledge the data provided by the USACE FRF, in particular, to Kent Hathaway who extracted the data from historical records that allowed the comparisons to be made on a timely basis. ISR has a continuing Co-operative R&D Agreement with the FRF.

REFERENCES

[1] H. Dankert J. Horstmann, and W. Rosenthal, Ocean Wind Fields Retrieved from Radar-Image Sequences, J. Geophys. Res.. Vol. 108, 2005.

[2] I.R.Young, , W. Rosenthal, F. Ziemer, A three-dimensional analysis of marine radar images for the determination of ocean wave directionality and surface currents, JGR, **90**, C1, pp. 1049-1059, 1985.

[3] D.B. Trizna, "Errors in Bathymetric Retrievals using Linear Dispersion In 3D FFT Analysis of Marine Radar Ocean Wave Imagery," IEEE Trans. Geosciences and Remote Sensing, **39**, pp. 2465-2469, 2001.

[4] C.M. Senet, J. Seemann, F. Ziemer, An iterative technique to determine the near surface current velocity from time series of sea surface images, Oceans '97, Halifax, 1997.

[5] Dugan, J.P., H.H. Suzukawa, C.P. Forsythe, M.S. Farber, Ocean wave dispersions surface measured with airborne IR imaging system, IEEE Trans. Geosciences and Remote Sensing, **34**, pp. 1282-1284, 1996.

[6] Dugan, J.P., C.P. Forsythe, H.H. Suzukawa, M.S. Farber, Bathymetry estimates from long range airborne imaging systems, Proc. 4th Int. Conf. On Remote Sensing for Marine and Coastal Environments, Orlando FL, 1997.

[7] Stockdon, H.F., and R.A. Holman, Estimation of wave phase speed and nearshore bathymetry from video imagery, J. Geophysical Res., **105**, pp. 22,015-22,034, 2000.

[8] McGregor, J.A., E.M Poulter, M.J. Smith, Switching system for single antenna operation of an S-band FMCW radar, IEE Proc. –Radar, Sonar, Navig, Vol. 141, pp 241-248, 1994.